ELSEVIER

Journal of Nuclear Materials 320 (2003) 184–193

journal of nuclear materials

www.elsevier.com/locate/jnucmat

Dissolution of magnetite using an environmentally friendly chelant: an electrochemical impedance spectroscopy study

A.M. Al-Mayouf *

Department of Chemistry, College of Science, King Saud University, P.O. Box 2455, Riyadh 11451, Saudi Arabia

Received 27 August 2002; accepted 11 February 2003

Abstract

Ethylenediaminedisuccinic acid (EDDS), a biodegradable substitute for EDTA, was used as a chelant for dissolving magnetite and magnetite formed on iron metal surface. Dissolution was found to increase in presence of ferrous ions and depend on pH of solution, concentration of ferrous ion, EDDS concentration, applied cathodic potential and temperature. The impedance spectrum for the dissolution of magnetite film formed on iron exhibited two time constants. The first at high frequency range is ascribed to the reductive dissolution of magnetite. It is very crucial to carry out the dissolution process at the appropriate temperature to insure complete removal of oxide layer.

1. Introduction

Iron is the most used metal in industry. During operation, especially when in contact with water, oxides are formed on its surface. It is usually caused by corrosion or from precipitation of soluble iron ions brought into the system by the makeup water. These oxides reduce the efficiency of water lines, boilers, cooling coils in water-cooled nuclear reactors and heat exchanger equipment and can speed under deposits corrosion. Therefore, removal of deposits will maximize thermal efficiency and capacity in steam generators and evaporators. Many solution formulations were developed to dissolve or to decontaminate metal surfaces from the oxide layers formed on the surface. Many workers have studied the dissolution of magnetite under reducing conditions. Reductants investigated include dithionite [1,2], thioglycolic acid [3], ascorbate [4], tris(bipyridyl)-Cr(II) [5], tris(picolinato)-V(II) [5,6]. Dissolution of magnetite by carboxylic acids in presence ferrous ions has been investigated. Among the carboxylic acids used were, nitrilotriacetic acid (NTA) [7], mercaptosuccinic acid, 3-merccaptopropionic acid and cysteine [8], oxalic acid [9,10], ethylenediaminetetraacetic acid (EDTA) [11]. Formulations that contain a reductant and a complexing agent like dithionate/EDTA [12], oxalic acid/EDTA [13], and ascorbic acid/citric acid/EDTA have been studied [14].

Commonly known procedures have been tested for their decontamination efficiency and selecting the appropriate procedure and optimum conditions is of great consideration. Among these procedures are AP-CITROX method (alkaline permanganate + citric acid + oxalic acid), AP-OX method (alkaline permanganate + oxalic acid), CITROX E method (citric acid + oxalic acid + EDTA), Can-Decon method and LOMI process that involves the use of vanadium (II) picolinate [15–17].

These formulations work either electrochemically or chemically as the dissolution process can be accelerated by the presence of higher levels of electrons or chelants ligands.

Chemical cleaning procedures which depend on suitable chelants are used to remove internal deposits, particularly iron based ones where strong mineral acids can corrode metals even in the presence of corrosion inhibitors. The use of chelating agents as cleaning chemicals for on-line and off-line cleaning seems to be gaining interest [18–24].

* Tel.: +966-1 4675959; fax: +966-1 4675992.
E-mail address: amayouf@ksu.edu.sa (A.M. Al-Mayouf).

0022-3115/03/$ - see front matter © 2003 Elsevier B.V. All rights reserved.
doi:10.1016/S0022-3115(03)00109-0

New chelants several of which chelate as effectively, if not better, than EDTA, but are largely more biodegradable have been developed [25]. Ethylenediaminedisuccinic acid (EDDS) is a biodegradable substitute for EDTA. It is more than 95% biodegradable than EDTA [26]. Photodegradation of EDDS is markedly faster than the degradation of EDTA both in filed and laboratory experiments [27]. EDDS is suggested as a promising substitute for EDTA in nuclear industry as it is as powerful chelating agent as EDTA and in the same time as a readily biodegradable alternative [28]. It will be also of great importance in chemical cleaning processes of boiler and metal surfaces in general if effluents after oxide dissolution are to be discharge without treatment.

Formulations that dissolve iron oxides by reductive dissolution are the most efficient ones [15]. These formulations contain reducing agents that can weaken the bonds between iron atoms in the iron oxide. This is achieved by reduction of surface Fe^{III} ions to Fe^{II}. This mechanism is called reductive dissolution and depends on the pH, temperature and redox potential. A wide range of reducing agents has been employed for the dissolution of iron oxides [29].

Most experimental studies have monitored the change in the level of iron released in solution from powdered iron oxides. The knowledge of the dissolution behavior of powdered magnetite is very useful to arrive at a suitable formulation for dissolving oxides. However, the data obtained using powdered oxide cannot be extrapolated to evaluate formulation for magnetite formed on iron surface. Iron metal is present in the latter and will take part in the dissolution of magnetite layer. Reductive dissolution of magnetite present on iron [29], carbon steel [14,30–34], stainless steel [13,35] and Inconel 600 [36] was reported. The contribution of underlying metal surface was found to depend on the thickness of the oxide layer and its condition. When the metal surface is exposed to the solution due to the presence of pores, cracks and other faults in the oxide layer or due to its reduced thickness, the corrosion reaction of the metal start to affect the oxide dissolution. In that case there is a possible galvanic coupling between the oxide and metal. The rate of dissolution of an oxide galvanically coupled to the metal decreases considerably and depends on the potential of oxide/metal couple [31,32].

Electrochemical impedance spectroscopy (EIS) is a powerful tool for the analysis of complex electrochemical systems. This technique is one of the few techniques available for in situ characterization of solid/liquid interface. Using EIS it is possible to evaluate in situ the influence of various parameters on the dissolution of iron oxide at different times [37].

EIS has been used in a few studies as an analytical tool to examine the growth of oxide layers at high temperatures on carbon steel and on 304 stainless steel [38,39]. It has also been used to study the iron pyrite/solution interface [40] and the removal of iron oxide deposited on Inconel 600 piping [36].

This paper describes the results obtained for the reductive dissolution of magnetite from magnetite crystal and from magnetite formed on iron surface in EDDS/Fe^{2+} couple using EIS. The effect of solution pH, concentration of EDDS and Fe^{2+}, applied cathodic potential and temperature was investigated to achieve high dissolution rate of magnetite. This work thus focused on two points: the use of EIS to obtain information for a quick evaluation of chemical formulations used to dissolve surface oxides and the use of more biodegradable substitute for EDTA.

2. Experimental

A crystal of magnetite (Fe_3O_4) in the form of a small cylinder with a diameter of 5 mm and 10 mm length was used. The electrode was prepared by attaching the magnetite crystal to a brass shaft with a conducting silver epoxy, and then it was mounted using Araldite resin with one surface exposed. The exposed surface was wet polished prior to each measurement using 600 and 1000 grit emery paper and then a suspension of 0.3 μm alumina powder on a polishing cloth. It was then washed and transferred quickly to the electrochemical cell.

Magnetite film was formed on iron discs 16-mm diameter and 2 mm thick. Initially the discs were polished using 600 and 1000-emery paper then washed with double distilled water. Finally, they were cleaned in an ultrasonic bath using acetone for 10 min. Iron discs were heated in an autoclave, which contains double distilled water adjusted to pH 10.5 with ammonia and excess hydrazine to oxidize iron discs at 230 °C for 30 days.

X-ray diffraction pattern of the film formed on iron surface confirmed the presence of magnetite by matching between magnetite film and standard lines calculated by FARHAN program [41]. Morphology of the grown oxide layer was also examined under an optical microscope and found to be very fine grained.

The linear sweep voltammetry measurements were carried out using a potentiostat controlled by a personal computer. All experiments were carried out using a three-electrode cell with saturated calomel electrode (SCE) and a platinum electrode as reference and counter electrodes, respectively. All potentials quoted are against SCE. Impedance measurements were carried out using a frequency response analyzer. The measurements were carried out either at open-circuit potential or at an applied cathodic potential using an ac potential sine wave signal of peak-to-peak amplitude of 10 mV. The frequency range used was 10 kHz to 0.01 mHz. Test solutions were prepared with doubly distilled water and analytical grade reagents. Ferrous ions were added as

ferrous ammonium sulfate. Solutions were degassed using high purity nitrogen for 1 h before and during each experiment.

3. Results

The dependence of magnetite reductive dissolution current density on applied potential in 0.5 M $NaClO_4$ + 0.02 M EDDS solution at pH 4.0 and 40 °C and at various scan rates is shown in Fig. 1. The peak current density increases with increasing scan rate while the peak potential is shifted slightly to more negative potential as the scan rate increases. This peak is attributed to the reduction of magnetite while part of the following current density is due to hydrogen evolution reaction [42]. This peak is comparable to the peak observed in 1 M ClO_4^- at similar potential and pH [43].

EIS was used to study the reductive dissolution of magnetite at open circuit potential in 0.5 M $NaClO_4$ + 0.01 M EDDS solution at 40 °C with 0.01 M Fe^{2+} ions at various pHs. Fig. 2 shows Nyquist plot of magnetite in 0.01 M EDDS + 0.01 M Fe^{2+} at 40 °C as a function of solution pH and open circuit potential. The plot consists of two depressed semicircles. However, in stationary solution Nyquist plot is composed of a semicircle followed by a diffusion tail in the lower frequency range. The semicircle in the high frequency range related to a charge transfer reaction is shown in both stationary and stirred solutions. This semicircle is due to reductive dissolution of magnetite. As we are interested in the dissolution process, then the charge transfer resistance and the constant phase element (R_2, Q_1) were obtained by fitting the impedance spectra using equivalent circuit (a) shown in Fig. 3. Q_1 is taken to be equal to the double layer capacitance. The dependence of R_2 and Q_1 on solution pH is shown in Fig. 4. It is clear from the plot that the dissolution rate is less at pH 1.5. R_2 decreases in going from pH 3.5 to 4.0. Q_1 is at its maximum value between pH 3.5 and 4.0 probably due to the high concentration of ions inside the double layer indicating more dissolution. The dependence of dissolution rate on pH is a result of several factors such as the influence of pH on the adsorption pre-equilibrium and the need for adsorbed protons adjacent to the reactive site [11].

The effect of EDDS and Fe^{2+} concentrations while keeping the ratio 1:1 on the dissolution of magnetite at pH 4.0 and 40 °C was studied using EIS. Nyquist plot at

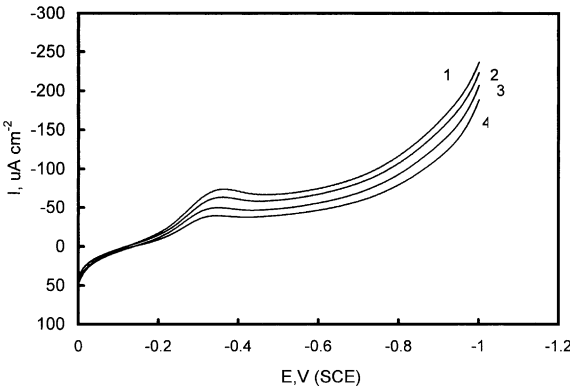

Fig. 1. Linear sweep voltammetry of magnetite in 0.5 M ClO_4^- + 0.02 M EDDS at pH 4 and various scan rates (1) 100, (2) 80, (3) 60 and (4) 40 mV/s.

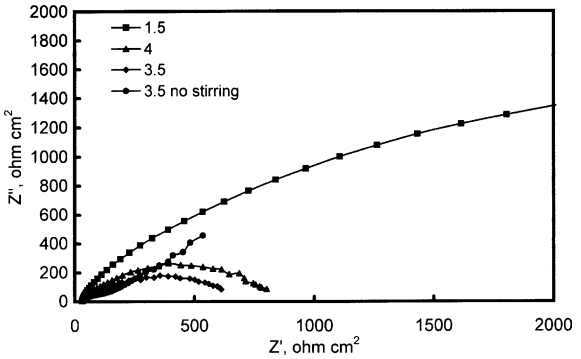

Fig. 2. Nyquist plot of magnetite in 0.01 M EDDS + 0.01 M Fe^{2+} at 40 °C and at different pH. ■, 1.5; ▲, 4.0; ◆, 3.5; ●, 3.5 no stirring.

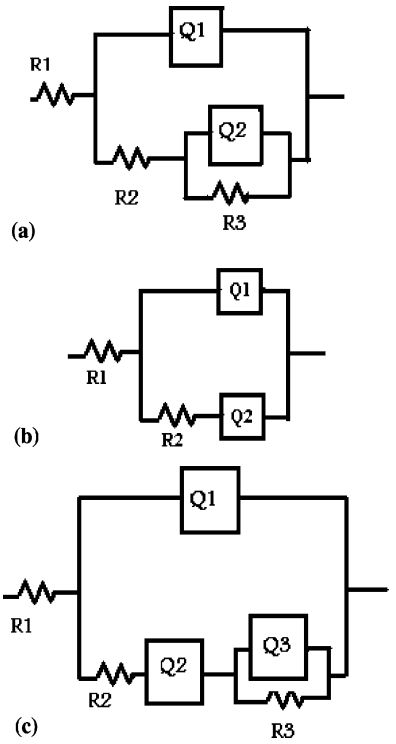

Fig. 3. Equivalent circuits used for EIS analysis.

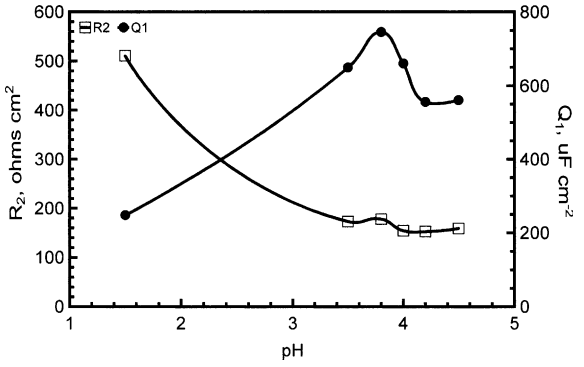

Fig. 4. Variation of R_2 and C_1 with solution pH for the dissolution of magnetite in magnetite in 0.5 M $NaClO_4$ + 0.01 M EDDS + 0.01 M Fe^{2+}.

various EDDS and Fe^{2+} concentrations has the same features shown in Fig. 2. It consists of two depressed semicircles and the sum of diameters of the two semicircles becomes smaller as the concentration increases. The resistance and capacitance of the first semicircle were obtained by fitting the impedance spectrum to equivalent circuit (a) in Fig. 3. Fig. 5 shows the variation of R_2 and Q_1 with the concentration of EDDS and Fe^{2+}. R_2 decreases as the concentration increases while Q_1 increases. R_2 is higher in absence of both EDSS and Fe^{2+}. This means that both of EDDS and Fe^{2+} play role in dissolving magnetite under conditions used in this study. The dissolution rate is related to the surface concentration of the reducing complex e.g. EDDS-Fe^{2+} [44]. The effect of Fe^{2+} concentration while keeping [EDDS] = 0.01 M on the dissolution of magnetite at pH 4.0 and 40 °C was studied using EIS. Nyquist plot at various Fe^{2+} concentration was similar to that shown in Fig. 2. The resistance and capacitance of the first semicircle were obtained by fitting the impedance spectrum to equivalent circuit (a) in Fig. 3. Fig. 6 shows

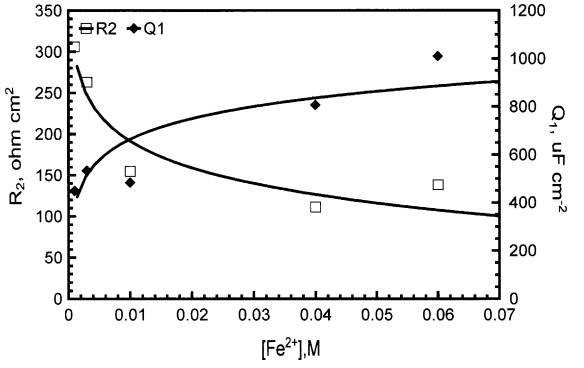

Fig. 5. Variation of R_2 and C_1 with concentration of EDDS and Fe^{2+} for the dissolution of magnetite in magnetite in 0.5 M $NaClO_4$ + 0.01 M EDDS at 40 °C. The ratio [EDDS]:[Fe^{2+}] is kept 1:1.

the variation of R_2 and Q_1 with the concentration of Fe^{2+}. R_2 decreases as the concentration increases while Q_1 increases. Comparison of Figs. 5 and 6 show that increasing [Fe^{2+}] resulted in more dissolution than that when both [EDDS] and [Fe^{2+}] were increased.

EIS was used to study the reductive dissolution of magnetite in 0.5 M $NaClO_4$ + 0.01 M EDDS solution at pH 4.0 and 40 °C as a function of applied potential.

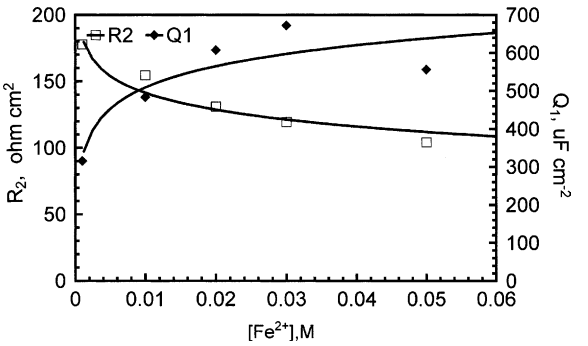

Fig. 6. Variation of R_2 and C_1 with concentration of Fe^{2+} for the dissolution of magnetite in magnetite in 0.5 M $NaClO_4$ + 0.01 M EDDS at 40 °C.

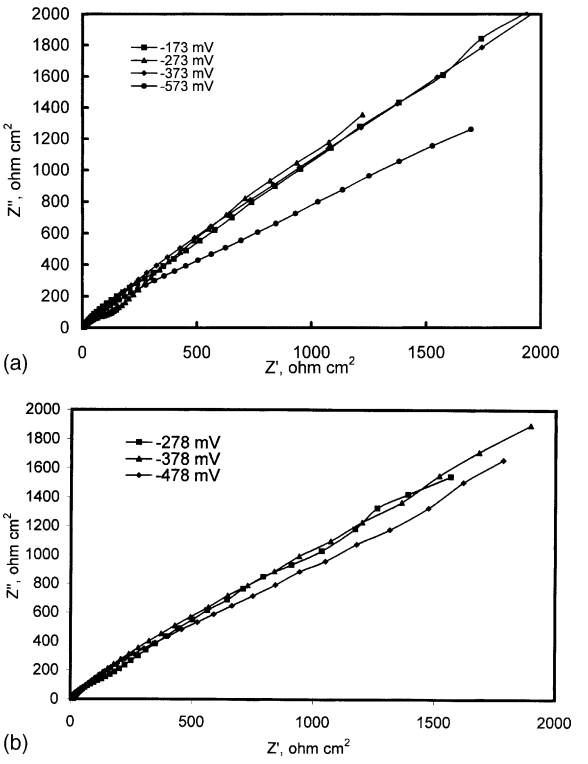

Fig. 7. (a): Nyquist plot of magnetite in stationary 0.01 M EDDS solution at pH 4.0 and 40 °C at different cathodic potentials. (b) Nyquist plot of magnetite in stirred 0.01 M EDDS solution at pH 4.0 and 40 °C at different cathodic potentials.

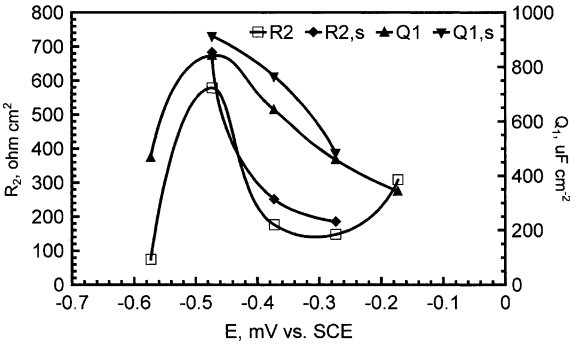

Fig. 8. Variation of R_2 and Q_1 with applied potential for magnetite dissolution in stirred and stationary 0.5 M $NaClO_4$ + 0.01 M EDDS at pH 4.0 and 40 °C.

The potential started from open circuit potential and increased in the negative direction with an increment of 100 mV. EIS spectra were recorded in stationary and stirred solutions. Fig. 7(a) and (b) show typical Nyquist plots of the reductive dissolution of magnetite in stationary and stirred solutions. The general features of plots are similar to those shown previously in 1 M $HClO_4$ at pH 4.0 [43] indicating that the dissolution process mechanism is the same in both solutions. The plot consists of an incomplete semicircle with a diffusion tail, which indicate that both electron transfer and diffusion processes control the dissolution of magnetite.

The effect of potential on the reductive dissolution was interpreted by fitting spectrum using the equivalent circuit (b) shown in Fig. 3. R_2 Q_1 combination represents the semicircle in Fig. 7(a) and (b). The value of R_2 and Q_1 are plotted in Fig. 8 as a function of potential for stirred and stationary solutions. It can be seen from the plot that R_2 has its lowest value around −0.30 V in both stirred and stationary solutions while Q_1 increases with applied potential and reached a maximum value for stationary solution around −0.5 V.

When both EDDS and Fe^{2+} are present in the solution the dissolution rate is greater than that observed in presence of EDDS only. Similar results were observed in an EIS study of magnetite in oxalate/Fe^{2+} system [43].

The dissolution of magnetite in 0.5 M $NaClO_4$ + 0.02 M EDDS solution at pH 4.0 in presence and absence of Fe^{2+} ions as a function of time and temperature was studied using EIS. In absence of added Fe^{2+} ions and at 40 °C Nyquist plot is composed of a semicircle and a diffusion tail and the shape of the plot does not depend

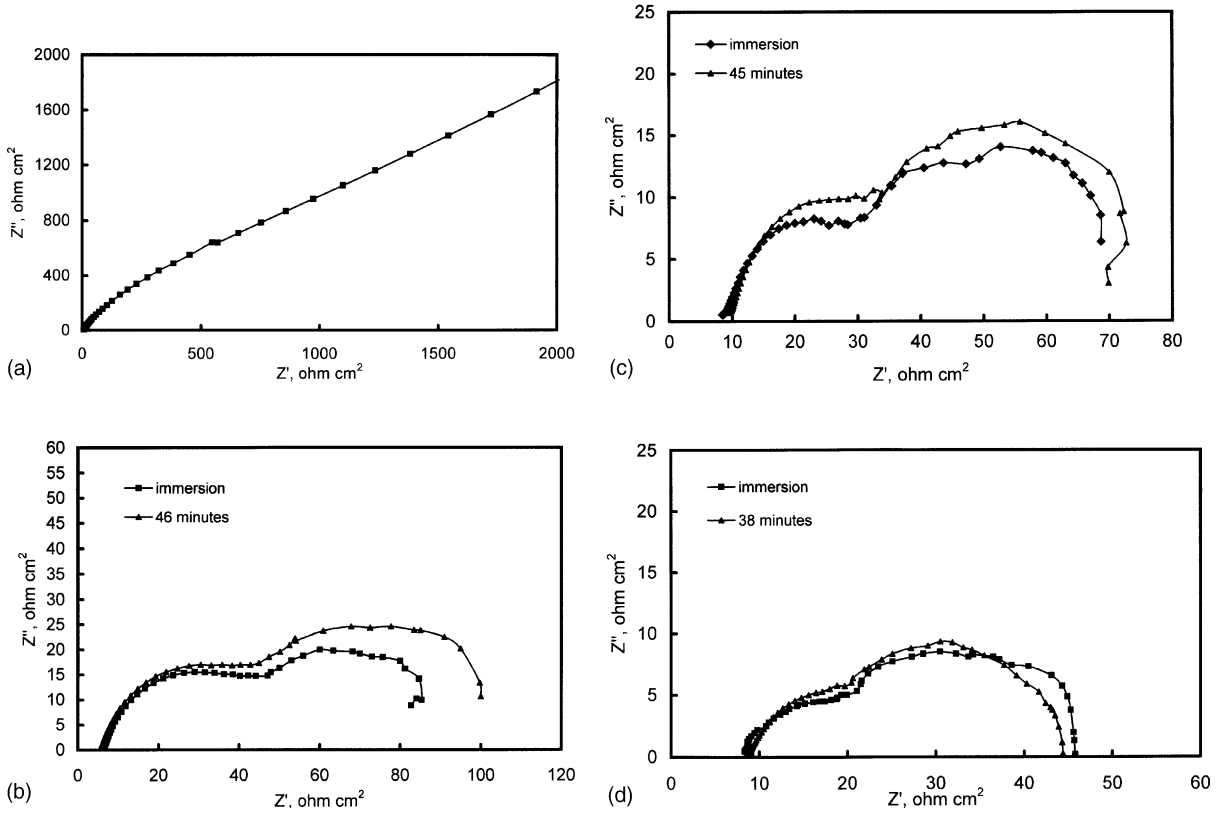

Fig. 9. Nyquist plot of magnetite dissolution in 0.5 M $NaClO_4$ + 0.02 M EDDS at pH 4.0. (a) At 40 °C in absence of added ferrous ions, (b) 0.02 M Fe^{2+} at 40 °C, (c) 0.02 M Fe^{2+} at 55 °C, (d) 0.02 M Fe^{2+} at 70 °C.

on dissolution time, Fig. 9(a). In presence of 0.02 M Fe^{2+}, the shape of the impedance spectrum changes to two flat semicircles, Fig. 9(b). At 55 and 70 °C, Nyquist plot still has the same shape with smaller diameter at higher temperature, Fig. 9(c) and (d). It is to be noticed that the diffusion tail in presence of added Fe^{2+} is not clear as it was in absence of Fe^{2+} ions but transformed to another semicircle. The recorded spectra were analyzed using the equivalent circuits (a) and (b) in Fig. 3. The potential of magnetite electrode was more negative in presence of added ferrous ions and its value was in the range −0.28 to −0.32 V. The potential of magnetite in absence of ferrous ions was about −0.11 V and became >0 after few measurements.

The charge transfer resistance is plotted at different temperatures in Fig. 10. In absence of Fe^{2+}, dissolution rate of magnetite is very low as the charge transfer resistance is high and decreases with time. But when Fe^{2+} is present in solution values of R_2 are smaller and depend on temperature. The change of R_2 with time is not linear as shown for magnetite in absence of Fe^{2+} ions. This may be explained by that the number of active sites do not change with time indicating steady state morphologies [45]. The time at which R_2 becomes nearly constant becomes shorter as temperature increases. This means that magnetite dissolves more at high temperature and thus temperature is considered one of crucial parameters for magnetite dissolution [31].

Iron released from magnetite at open circuit potential was chemically determined using atomic absorption analysis and in the same time measuring the potential and EIS of magnetite as a function of time in 0.5 M $NaClO_4$ + 0.02 M EDDS solution at pH 4.0 in presence and absence of 0.02 M Fe^{2+} ions. The average potential measured for magnetite was −0.13 V in absence of ferrous ions where it was −0.31 V in its presence. The amount of released iron increased linearly with dissolution time and it is higher in presence of ferrous ions. After analyzing the EIS spectra measured at various times, the charge transfer resistance of the dissolution process was found to have very high value in absence of ferrous ions. The resistance decreased in the first stage then became nearly constant. This means that the dissolution process occurs at constant rate and the amount of iron released is potential dependent, Fig. 11.

The dissolution of magnetite film formed on iron discs was studied using EIS in 0.5 M $NaClO_4$ + 0.01 M EDDS solution at pH 4.0 in presence of Fe^{2+} ions as a function of time and temperature. The Nyquist plot of magnetite film over iron at 55 °C and in presence of 0.02 M Fe^{2+} and at various times is shown in Fig. 12(a).

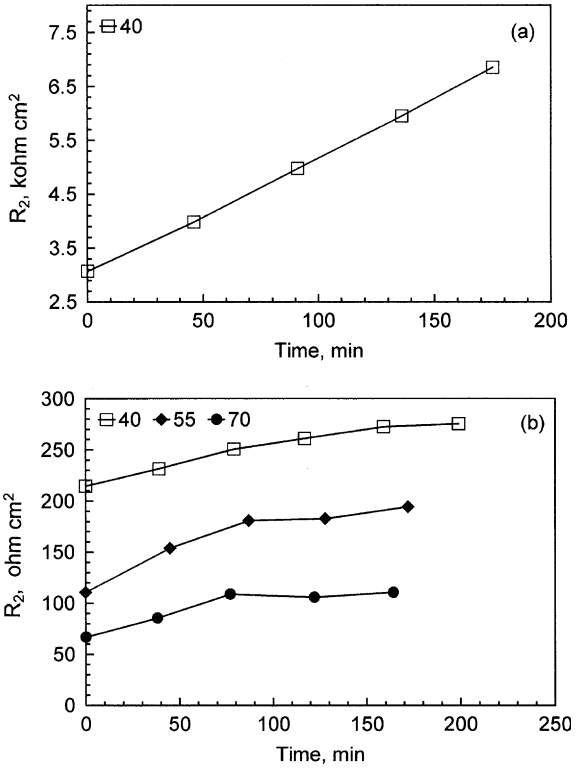

Fig. 10. The dependence of R_2 for the dissolution of magnetite on time and temperature in 0.5 M $NaClO_4$ + 0.02 M EDDS at pH 4.0 (a) in absence of Fe^{2+}; (b) in presence of 0.02 M Fe^{2+}.

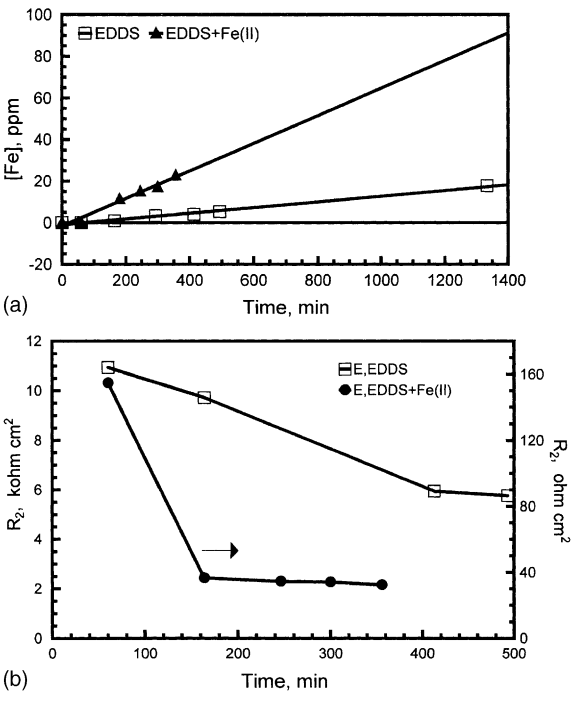

Fig. 11. (a) Dependence of iron released from magnetite in 0.5 M $NaClO_4$ + 0.02 M EDDS at pH 4.0 on time. (b) Dependence of R_2 on dissolution time during iron release from magnetite in the same solution.

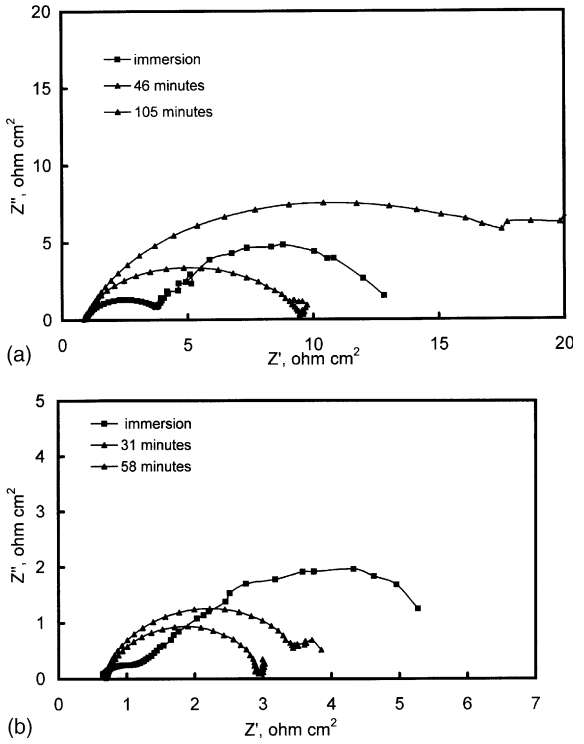

Fig. 12. Nyquist plots for iron with magnetite film in 0.5 M $NaClO_4$ + 0.02 M EDDS + 0.02 M Fe^{2+} at pH 4.0 as a function of time. (a) 55 and (b) 70 °C.

Initially, Nyquist plot consists of two semicircles similar to that displayed in Fig. 9(c) for magnetite at the same conditions. In the next measurements the shape of Nyquist plot consists of one semicircle. The diameter of the semicircle becomes smaller at longer dissolution times. The same features were also observed at 70 °C i.e. two semicircles on Nyquist plot initially then one semicircle afterward with the diameter of semicircle much less than that shown at the lower temperature, Fig. 12(b).

The behavior of iron was also investigated in the same solution at 70 °C. Fig. 13 shows Nyquist plot of iron, which displays a semicircle and an inductive loop at the low frequency. It can be seen that the spectra presented show at least two time constants. The first time constant recorded at higher and medium frequencies is depressed semicircles where the properties of metal/solution interface are particularly reflected, indicating that iron is dissolving. The second time constant at the lower frequency range is explained by the adsorption of reaction product at the metal/solution interface. When comparing the behavior of iron with magnetite film over it and that of polished iron, it can be concluded that at least the first time constant in Figs. 12(a), (b) and 13 is due to the dissolution of magnetite. The acquired potential of the specimen supports this

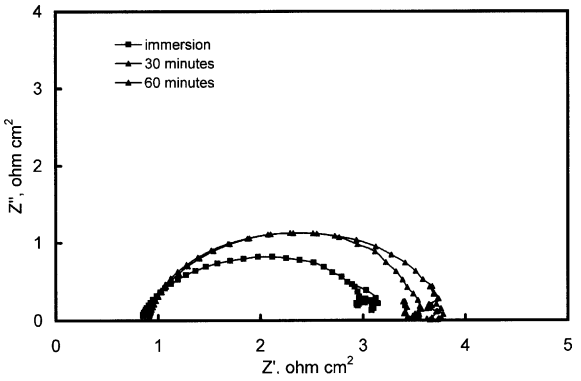

Fig. 13. Nyquist plots for iron in 0.5 M $NaClO_4$ + 0.02 M EDDS + 0.02 M Fe^{2+} at pH 4.0 and 70 °C as a function of time.

conclusion, which was first in the range of that of magnetite at the same conditions, then the potential drift quickly towards that of polished iron in the same solution.

The first impedance spectrum recorded for iron with magnetite film on it was analyzed using the equivalent circuit (c) in Fig. 3. Three time constants can be seen on that spectrum, two semicircles with the additional Q_2 in the middle. The resistances of the first time constant for the dissolution of magnetite on iron and for dissolution of iron as a function of time are depicted in Fig. 14. It can be seen from the figure that R_2 for the dissolution of magnetite on iron at 55 and 70 °C is low compared to that for iron. This is probably due to the effect of the iron substrate dissolution, which enhances the dissolution of oxide layer [31]. Then R_2 increase reaching a maximum then start to decrease after that noting that R_2 at 55 °C is lower that that at 70 °C. The change of R_2 with time indicates that the magnetite film was completely removed at 70 °C as its value is almost equal to that for iron. After measurement, the oxide film on the

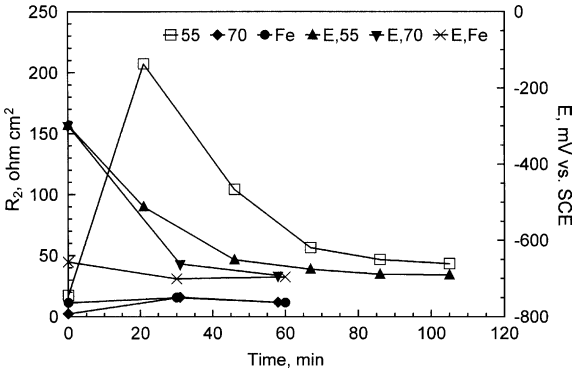

Fig. 14. Variation of charge transfer resistance (R_2) of the dissolution process for iron and iron with magnetite film as a function of time.

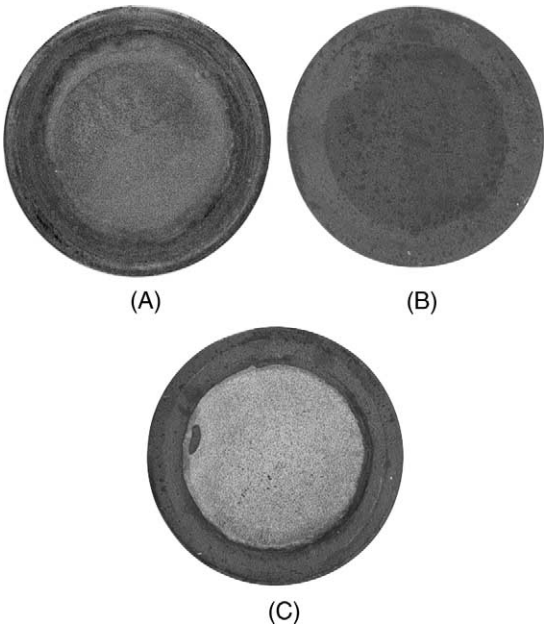

Fig. 15. Photos of iron samples after exposure to 0.5 M $NaClO_4$ + 0.02 M EDDS + 0.02 M Fe^{2+} solution, pH 4.0. (A) Polished iron at 70 °C after 60 min, (B) magnetite covered iron at 55 °C after 105 min, (C) magnetite covered iron at 70 °C after 58 min.

specimen was found to be completely removed and possibly some of the base metal, Fig. 15.

4. Discussion

The results of magnetite reductive dissolution in presence of EDDS with/or without Fe^{2+} ions at open circuit potential or with applied cathodic potential are similar to the results obtained in a previous study [43] although the rate may be not the same.

The dissolution mechanism involves the three different steps given in the oxalate/without Fe^{2+} system namely, adsorption of organic ligand on magnetite surface, non-reductive dissolution and reductive dissolution by EDDS/Fe^{2+} complex [46]. The operation of non-reductive dissolution of magnetite depends on the composition of the solution and temperature [46]. Non-reductive dissolution is a simple desorption process that removes reactive sites of the oxide surface:

$$\equiv Fe^{III}\text{–}OH^{+} + EDDS^{2-} + H^{+} \leftrightarrow [\equiv Fe^{III}\text{---}EDDS]^{2-} + H_2O \quad (1)$$

$$[\equiv Fe^{III}\text{---}EDDS]^{2-} + H^{+} \rightarrow [\equiv Fe^{3+}\text{---}EDDS]^{+}_{(aq)} + H^{+} \quad (2)$$

This process is usually slow at low temperature but becomes significant at high temperatures. This mechanism is operative in this study when Fe^{2+} is not present in solution, which is characterized by dissolution process with high charge transfer resistance and more positive potential of magnetite electrode.

As mentioned earlier, the reductive dissolution involves electron transfer from an adsorbed species to surface Fe^{III} [47,48]. The adsorbed species may be present in solution if Fe^{2+} ions were initially added to the solution. In that case the rate of dissolution is high with no induction period. If no Fe^{2+} ions are present in solution then Fe^{2+} ions will be generated in the solution from surface Fe^{II} ions. This is a slow process and until sufficient EDDS-Fe^{2+} complex is formed in solution the rate of dissolution is low:

$$\equiv Fe^{III} + [EDDS\text{–}Fe^{2+}]^{2-} \leftrightarrow \equiv Fe^{III}\text{---}[EDDS\text{–}Fe^{2+}]^{2-} \quad (3)$$

$$\equiv Fe^{III}\text{---}[EDDS\text{–}Fe^{2+}]^{2-} \rightarrow \equiv Fe^{II}\text{---}[EDDS\text{–}Fe^{3+}]^{-} \quad (4)$$

$$\equiv Fe^{II}\text{---}[EDDS\text{–}Fe^{3+}]^{-} \rightarrow \equiv Fe^{II} + [EDDS\text{–}Fe^{3+}]^{-} \quad (5)$$

$$\equiv Fe^{II} \rightarrow Fe^{2+}_{(aq)} \quad (6)$$

Iron base metal has been found to aid the dissolution of magnetite in according to the following scheme [14,31,33,34]:

$$Fe\ (\text{base metal}) \rightarrow Fe^{2+} + 2e^{-} \quad (7)$$

$$Fe_3O_4 + 8H^{+} + 2e^{-} \rightarrow 3Fe^{2+} + 4H_2O \quad (8)$$

$$Fe_3O_4 + 8H^{+} + Fe \rightarrow 4Fe^{2+} + 4H_2O \quad (9)$$

The iron base metal will dissolve by an anodic reaction whereas magnetite will dissolve by a cathodic reaction at their respective potentials. At the pH used in this study and at such potentials the dissolution of metal is controlled by hydrogen evolution reaction, which is the slow reaction in the base metal corrosion process [14,31,32]:

$$2H^{+} + 2e \rightarrow H_2 \quad (10)$$

The potential of oxide-covered iron is a mixed potential and it is in the range of −600 to −700 mV (SCE). Magnetite at the same conditions has a potential of about −300 mV (SCE). There is a possibility of galvanic

coupling between the potential of dissolving oxide and base metal [49]. This is evident from the change of observed potential with dissolution time. The drift to more negative potential indicates that dissolution of iron becomes predominant with time even if magnetite is still not completely dissolved. Further evidence comes from the shape of Nyquist plots of magnetite filmed iron at longer time as the two semicircles at the commencement of the experiment become one semicircle and the same time the potential moves to more negative values. Results shown in Figs. 12(a), (b) 13(b) and 15(B) show that although one semicircle is present on Nyquist plot at 55 °C, R_2 is higher than that of the first measurement and the removal of oxide is not complete. This means that the oxide layer becomes porous with progress of dissolution time, which enable the solution to reach the base metal and cause it to dissolve. However, this does not mean that both reductive dissolution of magnetite and corrosion of metal take place simultaneously. Complete dissolution of magnetite film occurs only at high temperature (70 °C) with significant corrosion of iron. In that case the use of corrosion inhibitor becomes a necessity [50].

5. Conclusions

The dissolution of magnetite in perchloric acid and in solutions containing EDDS/Fe^{II} was studied using electrochemical methods particularly EIS. The dissolution process was dependent on the applied cathodic potential.

EDDS a biodegradable substitute for EDTA was used to dissolve magnetite from a single crystal and from a magnetite film formed on iron surface. The dissolution rate was found to depend on the concentration of EDDS, Fe^{2+}, pH, applied potential and temperature. The rate of dissolution was enhanced by the presence of iron substrate, which aided the dissolution. EIS was capable to differentiate between the dissolution of magnetite film and iron metal.

The results obtained by in situ EIS measurement and after comparison with other results in the literature suggest that this method is suitable for quick evaluation of chemical formulations used to dissolve surface oxides in boilers and other heat exchangers.

Acknowledgements

The author acknowledges King Abdulaziz City for Science and Technology (KACST) for financial support under project LB-5-47. The author thanks the Department of Chemistry and Research Center for the use of their facilities.

References

[1] O.P. Mehra, M.L. Jackson, Clays Clay Miner. 7 (1960) 317.
[2] I.H.M. van Oorschot, M.J. Dekkers, Earth Planet Sci. Lett. 167 (1999) 283.
[3] E. Baumgartner, M.A. Blesa, A.J.G. Maroto, J. Chem. Soc. Dalton Trans. I (1982) 1649.
[4] M.D.S. Afonso, P.J. Morando, M.A. Blesa, S. Banwart, W. Stumm, J. Colloid, Interface Sci. 138 (1990) 74.
[5] M. Segal, R.M. Sellers, J. Chem. Soc. Chem. Commun. (1980) 991.
[6] G.C. Allen, C.K. Kirby, R.M. Sellers, J. Chem. Soc. Trans. 1 84 (1988) 355.
[7] M. del V. Hidalgo, N.E. Hatz, A.J.G. Maroto, M.A. Blesa, J. Chem. Soc. Trans. 1 84 (1988) 9.
[8] E.B. Borghi, P.J. Morando, M.A. Blesa, Langmuir 7 (1991) 1652.
[9] M.A. Blesa, H.A. Marinovich, E.C. Baumgartner, A.J.G. Maroto, Inorg. Chem. 26 (1987) 3713.
[10] M. Taxiarchou, D. Panias, I. Paspaliaris, A. Kontopoulos, Trans. Inst. Min. Metall. Sect (C) 107 (1998) C37.
[11] E.B. Borghi, A.E. Regazzoni, A.J.G. Maroto, M.A. Blesa, J. Colloid, Interface Sci. 130 (1989) 299.
[12] E.H. Rueda, M.C. Ballesteros, R.L. Grassi, M.A. Blesa, Clays Clay Min. 40 (1992) 575.
[13] D.W. Shoesmith, D.S. Mancey, D.C. Doern, M.G. Bailey, Corrosion Sci. 45 (1989) 149.
[14] M. Shailaja, S.V. Narasimhan, J. Nucl. Sci. Technol. 30 (1993) 524.
[15] J. Severa, J. Bár, Handbook of Radioactive Contamination and Decontamination, Elsevier, New York, 1991.
[16] J. Torok, in: Decontamination of nuclear facilities, International joint topical meeting ANS-CAN, Niagara Falls, 1892.
[17] D. Bradbury, M.G. Segal, R.M. Sellers, T. Swan, C.J. Wood, in: Decontamination of nuclear facilities, International joint topical meeting ANS-CAN, Niagara Falls, 1892.
[18] R.I. Kaplan, E.W. Ekis Jr., Mater. Performance (November) (1984) 40.
[19] A. Abdul-Latif, S.H. Al-Madfai, A.N. Ghanim, Ind. Eng. Chem. Res. 27 (1988) 1548.
[20] R. Brouillette, R. Kerridge, G. Millette, Annual Meeting-Technical Section, Canadian Pulp and Paper Association, Preprints. Published by Canadian Pulp and Paper Assoc, Montreal, Que., Canada, p. 153.
[21] J. Bosholm, Kerntechnik 58 (1993) 37.
[22] V.S. Vorob'eva, Coke Chem. 5 (1991) 38.
[23] R.A. Hoffmann, A.J. Freedman, Mater. Performance (February) (1997) 56.
[24] D.H. Hur, H.S. Chung, U.C. Kim, J. Nucl. Mater. 224 (1995) 179.
[25] D. Williams, Chem. Brit. 4 (1998) 48.
[26] R. Takahashi, N. Fujimoto, M. Suzuki, T. Endo, Biosci. Biotech. Biochem. 61 (1997) 1957.
[27] S. Metsarinne, T. Tuhkanen, R. Aksela, Chemosphere 45 (2001) 949.
[28] P.W. Jones, D.R. Williams, Appl. Radiation Isotopes 54 (2001) 587.
[29] R.M. Cornell, U. Schwertmann, The Iron Oxides, Structure, Properties, Reactions, Occurrence and Uses, VCH, Weinheim, Germany, 1996.

[30] M.J. Pryor, U.R. Evans, J. Chem. Soc. (1950) 1259.
[31] A.A.M. Prince, S. Velmurugan, S.V. Narasimhan, C. Ramesh, N. Murugesan, P.S. Raghavan, R. Gopalan, J. Nucl. Mater. 289 (2001) 281.
[32] I.H. Plonski, J. Appl. Electrochem. 27 (1997) 1184.
[33] D.W. Shoesmith, W. Lee, D.G. Owen, Power Ind. Res. 1 (1981) 253.
[34] D.W. Shoesmith, T.E. Rummerym, W. Lee, D.G. Owen, Power Ind. Res. 1 (1981) 43.
[35] E.B. Borghi, S.P. Ali, P.J. Morando, M.A. Blesa, J. Nucl. Mater. 229 (2001) 115.
[36] J. Abellà, J. Barceló, L. Victori, Corrosion Sci. 40 (1998) 1561.
[37] P.A. Christensen, A. Hamentt, Techniques and Mechanisms in Electrochemistry, Blackie Academic & professional, London, 1994.
[38] J.J. Senkevich, D.A. Jones, I. Chatterjee, Corrosion Sci. 42 (2000) 201.
[39] Y.J. Kim, Corrosion 56 (2000) 389.
[40] J. Pang, A. Briceno, S. Chander, J. Electrochem. Soc. 137 (1990) 3447.
[41] K. Farhan, Powder Diffraction 14 (1999) 16.
[42] D.S. Mancey, D.W. Shoesmith, J. Lipkowski, A.C. McBride, J. Noël, J. Electrochem. Soc. 140 (1993) 637.
[43] A.M. Al-Mayouf, Corrosion 58 (2002) 519.
[44] M.A. Blesa, A.J.G. Maroto, A.E. Regazzoni, Trends Inorg. Chem. 3 (1993) 25.
[45] H. Tamura, N. Ito, M. Kitano, S. Takasaki, Corrosion Sci. 43 (2001) 1675.
[46] D. Panias, M. Taxiarchou, I. Paspaliaris, A. Kontopoulos, Hydrometallurgy 42 (1996) 257.
[47] M.A. Blesa, in: Decontamination of nuclear facilities, International joint topical meeting ANS-CAN, Niagara Falls, 1982.
[48] E. Baumgartnerm, M.A. Blesa, H.A. Marinovich, A.J. Maroto, Inorg. Chem. 22 (1983) 2226.
[49] N. Sato, Corrosion Sci. 42 (2000) 1957.
[50] B. Buecker, Mater. Performance (January) (2001) 52.